Supplementary information for

The role of interfacial tension in the size-dependent phase separation of atmospheric aerosol particles.

Ryan Schmedding[1] and Andreas Zuend[1]

[1]Department of Atmospheric and Oceanic Sciences, McGill University, Montreal, Canada

Correspondence: Andreas Zuend (andreas.zuend@mcgill.ca)

Table S1. List of abbreviations used in this work and their meanings.

Abbreviation	Meaning
AIOMFAC	Aerosol Inorganic–Organic Mixtures Functional groups Activity Coefficients
CCN	Cloud Condensation Nucleus
CSOA	Complex Secondary Organic Aerosol mixture
IFE	Interfacial Energy
LLE	Liquid–Liquid Equilibrium
LL	Liquid–Liquid
LLPS	Liquid–Liquid Phase Separation
OIR	Organic-to-Inorganic dry mass Ratio
PM	Particulate Matter
RH	Relative Humidity
SOA	Secondary Organic Aerosol
SRH	Separation Relative Humidity

Table S2: List of mathematical symbols used in this work and their meanings.

Category	Symbol	Meaning	Units
Mathematical Variables	A	area of the surface	$\mathrm{m^2}$
	$\mathscr{A}$	partial molar area	$\mathrm{m^2\,mol^{-1}}$
	D	diameter	m
	G	Gibbs energy	J
	M	molar mass	$\mathrm{kg\,mol^{-1}}$
	n	number of moles	mol
	P	pressure	Pa
	R	universal gas constant	$\mathrm{J\,mol^{-1}\,K^{-1}}$
	r	radius	m
	S	entropy or saturation ratio (depending on context)	$\mathrm{J\,K^{-1}}$ or $-$
	T	temperature	K
	U	internal energy	J
	V	system volume	$\mathrm{m^3}$
	$\mathscr{V}$	molar volume	$\mathrm{m^3\,mol^{-1}}$
	x	mole fraction	$-$
Greek Letter Variables	η	exponential scaling factor for interfacial composition	-
	γ	activity coefficient	-
	δ	thickness of Guggenheim surface phase	m
	ι	length of a three-phase boundary line	m
	μ	chemical potential	$\mathrm{J\,mol^{-1}}$
	ρ	density	$\mathrm{kg\,m^{-3}}$
	σ	surface or interfacial tension	$\mathrm{J\,m^{-2}}$
	τ	line energy at a three-phase boundary	$\mathrm{J\,m^{-1}}$
	ε	fraction of the total particle amount of species partitioned to the surface phase (surface fraction)	-
Superscripts and Subscripts	α	inorganics-rich phase	$-$
	β	organics-rich phase	$-$
	b	bulk phase	$-$
	disp	dispersion force based calculation	$-$
	el	inorganic electrolyte species	$-$
	G	Gas-phase property	$-$

i	chemical component or species index	—
$\circ$	standard or reference state	—
ϕ	phase index or semi-empirical Girifalco–Good equation parameter (depending on context)	—
ls	Liquid–Surface	—
p	particle	—
′	liquid–liquid-interface-corrected property	—
s	surface phase	—
sat	saturation	—
suppr	suppression limit	—
tot	total	—
vf	volume-fraction-based	—
w	water	—
$\star$	measurable	—

Table S3: Reference pure-component liquid-state surface tension values at 298 K (σ_i°) and dry particle mass fractions for the systems discussed in this work. Organic compounds of unknown σ_i° due to lack of experimental data were assigned $\sigma_i^\circ = 35\,\mathrm{mJ\,m^{-2}}$. $\sigma_w^\circ = 71.98\,\mathrm{mJ\,m^{-2}}$ at 298 K (Vargaftik et al., 1983).

Compound	Molar Mass [kg mol^{-1}]	Dry Mass Frac [–]	σ_i° [mJ m^{-2}]	Reference
Ethanol	0.046069	1.00*	22.1	Khattab et al. (2012)
NaCl	0.058443	1.00*	174.0	Dutcher et al. (2010)
PEG-300 n5	0.282332	0.181	43.6	Ai et al. (2022)
PEG-300 n6	0.326384	0.168	43.6	Ai et al. (2022)
$(NH_4)_2SO_4$	0.132139	0.651	184.5	Dutcher et al. (2010)
Suberic acid	0.174156	0.537	45.0	Hyvärinen et al. (2006)
$(NH_4)_2SO_4$	0.132139	0.463	184.5	Dutcher et al. (2010)
PEG-400 n7	0.3704376	0.155	44.5	Sequeira et al. (2019)
PEG-400 n8	0.4144904	0.345	44.5	Sequeira et al. (2019)
$(NH_4)_2SO_4$	0.132139	0.500	184.5	Dutcher et al. (2010)
1,2,6-Hexanetriol	0.134172	0.504	48.5	Sigma-Aldrich (2006)
$(NH_4)_2SO_4$	0.132139	0.496	184.5	Dutcher et al. (2010)
Benzene	0.078108	0.57-0.9999[†]	28.75	Součková et al. (2013)
NaCl	0.058443	0.0001-0.43[†]	174.5	Dutcher et al. (2010)
Dodecane	0.148152	0.67-0.9999[†]	25.0	Koller et al. (2017)
KCl	0.074551	0.0001-0.33[†]	155.4	Dutcher et al. (2010)
Benzene	0.078108	0.55-0.9999[†]	28.75	Součková et al. (2013)
Methanol	0.032042	0.0001-0.45[†]	22.5	Jasper (1972)
1,2,5,8-Octanetetrol	0.178224	0.0505	35.0	–
2-Methylglutaric acid	0.146104	0.0504	50.0	Hyvärinen et al. (2006)[‡]
3,5-Dihydroxybenzoic acid	0.142054	0.0464	70.5	Tuckermann and Cammenga (2004)[§]
3-Hydroxybenzoic acid	0.138082	0.0252	70.5	Tuckermann and Cammenga (2004)
3-Methyladipic acid	0.160130	0.0504	35.0	Riipinen et al. (2007)[¶]
Levoglucosan	0.162122	0.0504	22.7	Topping et al. (2007)
Malic acid	0.134052	0.0504	50.0	Hyvärinen et al. (2006)
Pinolic acid	0.186226	0.0067	35.0	–
Pinonic acid	0.196176	0.0140	66.1	Varga et al. (2007)
Succinic acid	0.118052	0.0504	47.5	Hyvärinen et al. (2006)
$(NH_4)_2SO_4$	0.132139	0.605	184.5	Dutcher et al. (2010)

C107OOH (MCM name)	0.200166	8.92×10^{-4}	35.0	–
Pinonic acid	0.184166	4.64×10^{-4}	66.1	Varga et al. (2007)
C97OOH (MCM name)	0.188174	9.65×10^{-3}	35.0	–
C108OOH (MCM name)	0.21613	0.37	35.0	–
Pinalic acid	0.170166	6.97×10^{-5}	35.0	–
Pinic acid	0.186166	3.05×10^{-2}	23.8	Topping et al. (2007)
C921OOH (MCM name)	0.204182	3.83×10^{-2}	35.0	–
C109OOH (MCM name)	0.200174	6.46×10^{-5}	35.0	–
C812OOH (MCM name)	0.158174	3.27×10^{-2}	35.0	–
10-Hydroxypinonic acid	0.206138	9.49×10^{-3}	66.1	Varga et al. (2007)[‖]
C811OH (MCM name)	0.158174	2.88×10^{-4}	35.0	–
C813OOH (MCM name)	0.206138	1.39×10^{-2}	35.0	–
Aldol dimer	0.368298	4.50×10^{-3}	35.0	–
Ester dimer	0.368306	1.80×10^{-2}	35.0	–
$(NH_4)_2SO_4$	0.132139	0.471	184.5	Dutcher et al. (2010)

[*] binary systems were run assuming the dry composition case is pure solute.

[†] the system was run at variable dry composition at fixed RH to replicate measurements.

[‡] estimated from structural similarity to glutaric acid.

[§] estimated from structural similarity to hydroxybenzoic acid.

[¶] estimated from structural similarity to adipic acid.
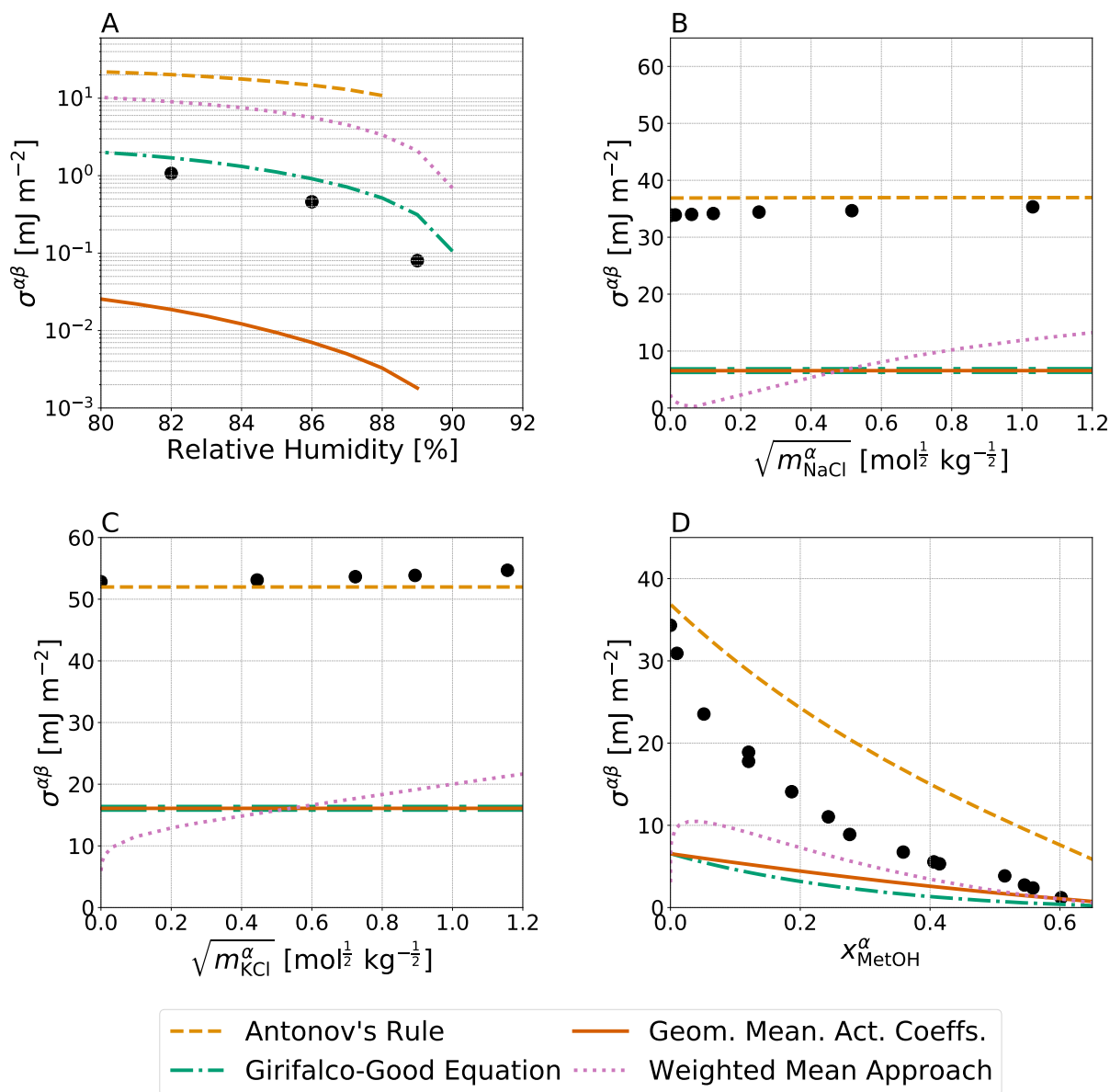
[‖] estimated from structural similarity to pinonic acid.

Figure S1. Predicted $\sigma^{\alpha\beta}$ with adjustments to $\sigma^{\circ}_{\text{org}}$ and $\sigma^{\circ}_{\text{el}} = \sigma^{\circ}_{\text{w}}$. $\sigma^{\circ}_{\text{PEG}-400}$, $\sigma^{\circ}_{\text{benzene}}$, and $\sigma^{\circ}_{\text{MetOH}} = 35$ mJ m^{-2} in subplots A, C, and D. In subplot D, $\sigma^{\circ}_{\text{dodecane}} = 20$ mJ m^{-2}. These values were selected to better fit Antonov's rule to the measured data for the systems shown in subplots B and C and to explore the sensitivity of the more miscible systems shown in subplots A and D to changes in $\sigma^{\circ}_{\text{org}}$ and $\sigma^{\circ}_{\text{el}}$.
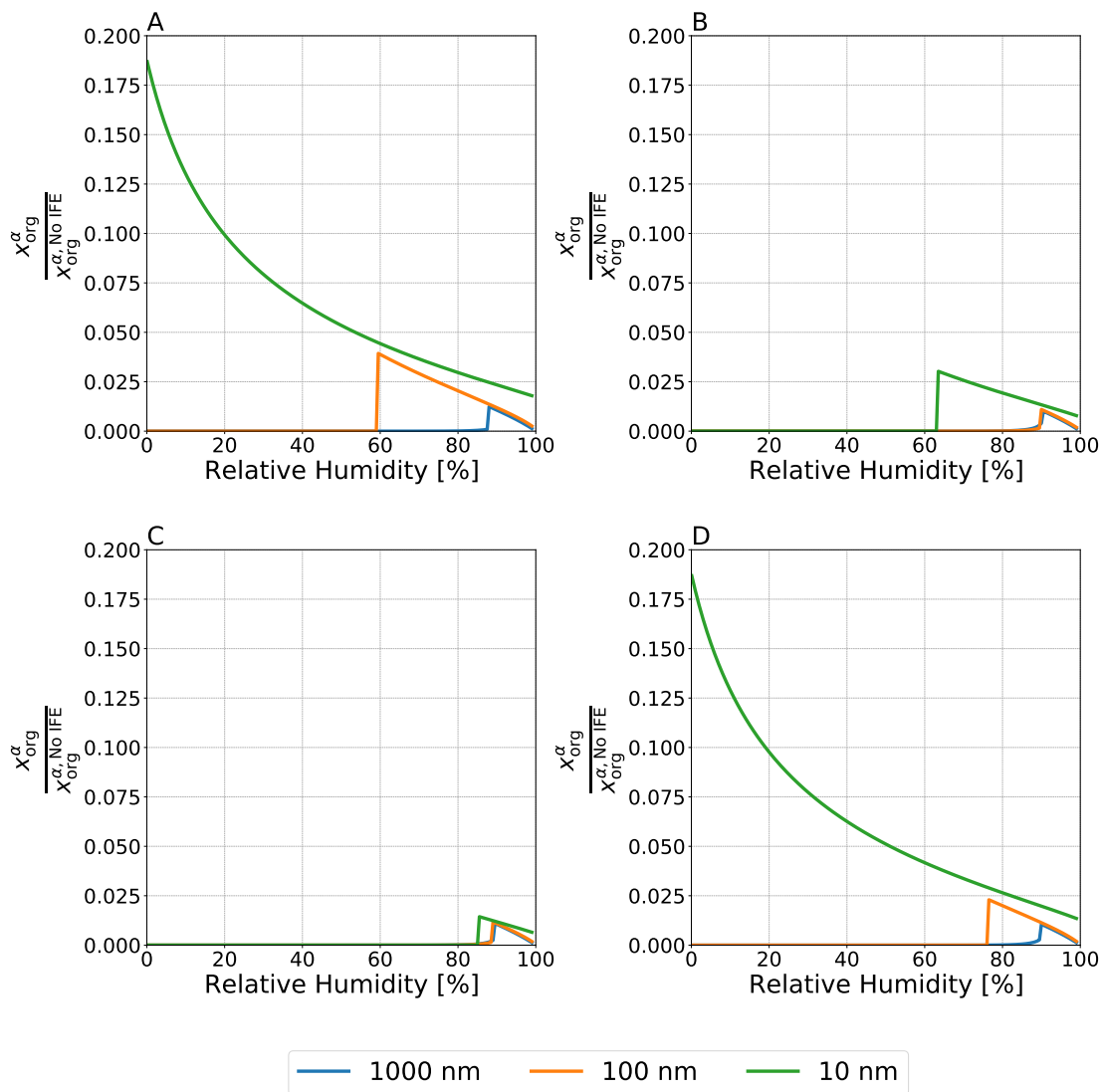
Figure S2. Normalized mole fraction of PEG-400 in the aqueous phase for water, PEG-400, and ammonium sulfate particles with dry diameters ranging from 10 nm to 1000 nm for (A) Antonov's rule, (B) the Girifalco–Good equation, (C) Butler equation with modified activity coefficients, and (D) the weighted mean interfacial composition approach.
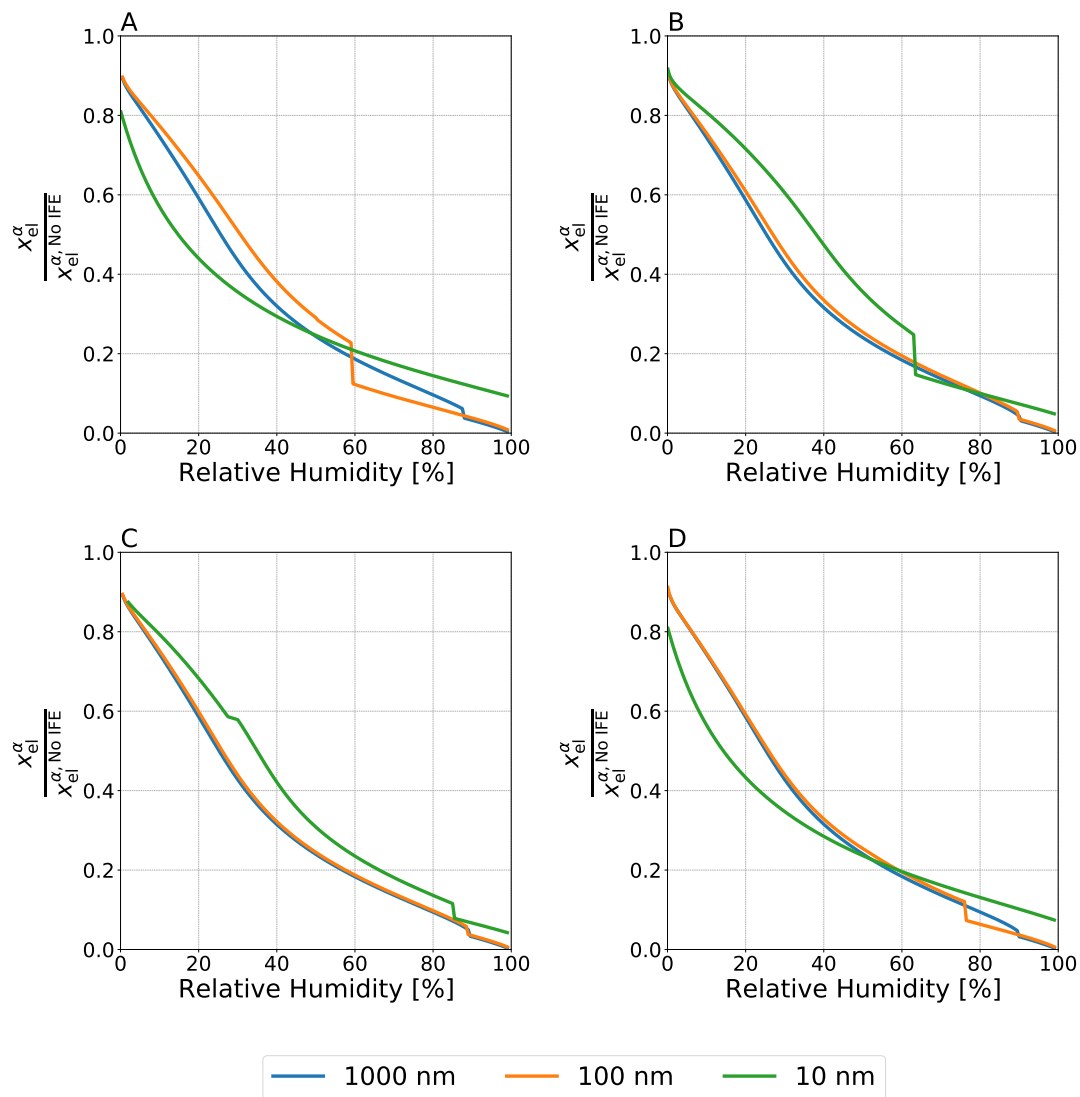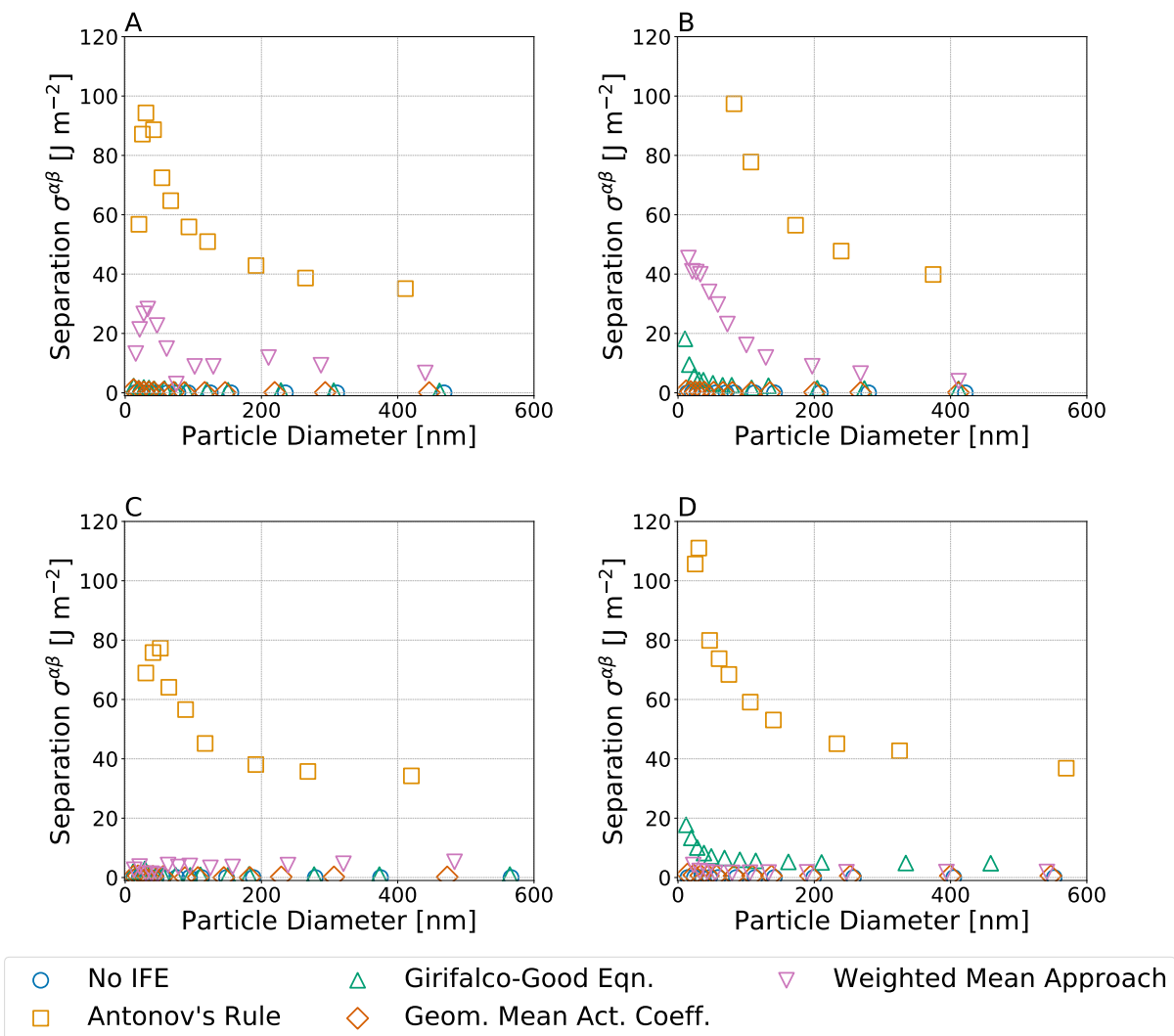
Figure S3. Normalized mole fraction of ammonium sulfate in the aqueous phase for water, PEG-400, and ammonium sulfate particles with dry diameters ranging from 10 nm to 1000 nm for (A) Antonov's rule, (B) the Girifalco–Good equation, (C) Butler equation with modified activity coefficients, and (D) the weighted mean interfacial composition approach.

Figure S4. Predicted $\sigma^{\alpha\beta}$ at the onset of LLPS upon dehumidification, shown for a range of particle (wet) diameters at $T = 298$ K. The systems shown are: (A) Water–PEG-300–ammonium sulfate, (B) water–1,2,6-hexanetriol–ammonium-sulfate, (C) water, a CSOA mixture with succinic acid and ammonium sulfate, and (D) water, α-pinene SOA surrogates, and ammonium sulfate. Distinct symbols refer to different approaches used for the LL interfacial tension estimations; see legend. For particles with stronger size-dependent onset of LLPS, there is less agreement among the predicted $\sigma^{\alpha\beta}$ at the onset of phase separation. At these sizes, complete partitioning of one species into the aqueous, organic, or surface phase leads to greater differences in the internal composition of the particle.
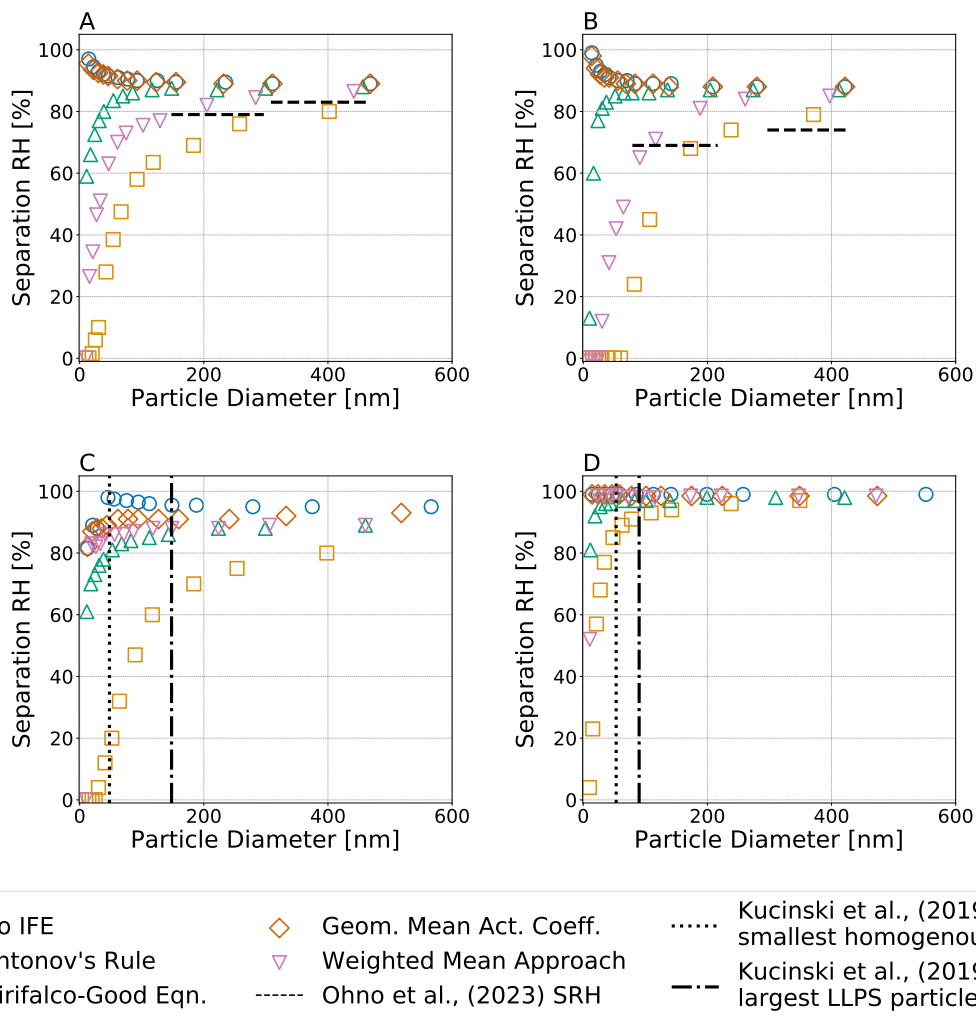
Figure S5. Predicted equilibrium separation RH versus particle wet diameter for particles of the same dry composition but different choices of interfacial tension treatment; see legend. In this case it is assumed that $\sigma^{ls} = 0$ and therefore $\sigma^{s\star} = \sigma^{s}$. Systems shown are: (A) water–PEG-300–ammonium-sulfate; (B) water–1,2,6-hexanetriol–ammonium-sulfate; (C) water–CSOA-with-succinic-acid–ammonium-sulfate; (D) water–α-pinene-SOA–ammonium-sulfate. Shown by dashed horizontal lines in (A, B) are measured equilibrium separation RH values by Ohno et al. (2023). Shown in (C, D) by vertical lines are the observed largest homogenous and smallest phases-separated particles as determined by Kucinski et al. (2019). All calculations were performed at 298 K.

References

Ai, J., Li, F., Zhang, J., and Wu, Z.: Density, viscosity, surface tension, and spectral analysis of polyethylene glycol 300 + 1,2-Propylenediamine binary liquid mixture, Journal of Molecular Liquids, 361, 119 579, https://doi.org/https://doi.org/10.1016/j.molliq.2022.119579, 2022.

5   Dutcher, C. S., Wexler, A. S., and Clegg, S. L.: Surface Tensions of Inorganic Multicomponent Aqueous Electrolyte Solutions and Melts, The Journal of Physical Chemistry A, 114, 12 216–12 230, https://doi.org/10.1021/jp105191z, pMID: 21043484, 2010.

Hyvärinen, A.-P., Lihavainen, H., Gaman, A., Vairila, L., Ojala, H., Kulmala, M., and Viisanen, Y.: Surface Tensions and Densities of Oxalic, Malonic, Succinic, Maleic, Malic, and cis-Pinonic Acids, Journal of Chemical & Engineering Data, 51, 255–260, https://doi.org/10.1021/je050366x, 2006.

10   Jasper, J. J.: The Surface Tension of Pure Liquid Compounds, Journal of Physical and Chemical Reference Data, 1, 841–1010, https://doi.org/10.1063/1.3253106, 1972.

Khattab, I. S., Bandarkar, F. S., Fakhree, M. A. A., and Jouyban, A.: Density, viscosity, and surface tension of water+ethanol mixtures from 293 to 323K, Korean Journal of Chemical Engineering, 29, 812–817, https://doi.org/10.1007/S11814-011-0239-6, 2012.

Koller, T. M., Klein, T., Giraudet, C., Chen, J., Kalantar, A., van der Laan, G. P., Rausch, M. H., and Fröba, A. P.: Liquid Viscosity and
15   Surface Tension of n-Dodecane, n-Octacosane, Their Mixtures, and a Wax between 323 and 573 K by Surface Light Scattering, Journal of Chemical & Engineering Data, 62, 3319–3333, https://doi.org/10.1021/acs.jced.7b00363, 2017.

Kucinski, T. M., Dawson, J. N., and Freedman, M. A.: Size-Dependent Liquid–Liquid Phase Separation in Atmospherically Relevant Complex Systems, The Journal of Physical Chemistry Letters, 10, 6915–6920, https://doi.org/10.1021/acs.jpclett.9b02532, pMID: 31638813, 2019.

20   Ohno, P. E., Brandão, L., Rainone, E. M., Aruffo, E., Wang, J., Qin, Y., and Martin, S. T.: Size Dependence of Liquid–Liquid Phase Separation by in Situ Study of Flowing Submicron Aerosol Particles, The Journal of Physical Chemistry A, 127, 2967–2974, https://doi.org/10.1021/acs.jpca.2c08224, pMID: 36947002, 2023.

Riipinen, I., Koponen, I. K., Frank, G. P., Hyvärinen, A.-P., Vanhanen, J., Lihavainen, H., Lehtinen, K. E. J., Bilde, M., and Kulmala, M.: Adipic and Malonic Acid Aqueous Solutions: Surface Tensions and Saturation Vapor Pressures, The Journal of Physical Chemistry A,
25   111, 12 995–13 002, https://doi.org/10.1021/jp073731v, pMID: 18044850, 2007.

Sequeira, M. C., Pereira, M. F., Avelino, H. M., Caetano, F. J., and Fareleira, J. M.: Viscosity measurements of poly(ethyleneglycol) 400 [PEG 400] at temperatures from 293 K to 348 K and at pressures up to 50 MPa using the vibrating wire technique, Fluid Phase Equilibria, 496, 7–16, https://doi.org/https://doi.org/10.1016/j.fluid.2019.05.012, 2019.

Sigma-Aldrich: Technical Bulletin AL-128, Tech. rep., Sigma-Aldrich Corporation, https://www.sigmaaldrich.com/deepweb/assets/
30   sigmaaldrich/product/documents/394/249/al_techbull_al128.pdf, 2006.

Součková, M., Klomfar, J., and Pátek, J.: Standard reference data for the air–liquid and vapor–liquid surface tension of benzene, Fluid Phase Equilibria, 356, 329–337, https://doi.org/https://doi.org/10.1016/j.fluid.2013.07.053, 2013.

Topping, D. O., McFiggans, G. B., Kiss, G., Varga, Z., Facchini, M. C., Decesari, S., and Mircea, M.: Surface tensions of multi-component mixed inorganic/organic aqueous systems of atmospheric significance: measurements, model predictions and importance for cloud acti-
35   vation predictions, Atmospheric Chemistry and Physics, 7, 2371–2398, https://doi.org/10.5194/acp-7-2371-2007, 2007.

Tuckermann, R. and Cammenga, H. K.: The surface tension of aqueous solutions of some atmospheric water-soluble organic compounds, Atmospheric Environment, 38, 6135–6138, https://doi.org/https://doi.org/10.1016/j.atmosenv.2004.08.005, 2004.

Varga, Z., Kiss, G., and Hansson, H.-C.: Modelling the cloud condensation nucleus activity of organic acids on the basis of surface tension and osmolality measurements, Atmospheric Chemistry and Physics, 7, 4601–4611, https://doi.org/10.5194/acp-7-4601-2007, 2007.

40 Vargaftik, N. B., Volkov, B. N., and Voljak, L. D.: International Tables of the Surface Tension of Water, Journal of Physical and Chemical Reference Data, 12, 817–820, https://doi.org/10.1063/1.555688, 1983.